




Article

Fast Energy Recovery During Motor Braking: Analysis and Simulation

Lin Xu ^{1,2}, Wengan Li ², Zenglong Zhao ²  and Fanyi Meng ^{2,*} 

¹ The 13th Research Institute, China Electronics Technology Group Corporation, Shijiazhuang 050051, China; xulin@cetc13.cn

² School of Microelectronics, Tianjin University, Tianjin 300072, China; 3020205026@tju.edu.cn (W.L.); zlzhao@tju.edu.cn (Z.Z.)

* Correspondence: meng.fanyi@gmail.com

Abstract

At present, environmental pollution is becoming more and more serious, and the energy problem is becoming more prominent. Energy-braking recovery can collect the mechanical energy lost in the traditional braking process and convert it into electricity or other forms of energy for vehicle reuse, thus reducing carbon emissions, achieving energy saving and emission reduction, and promoting green development. Based on this, this paper studies the energy-braking recovery method. The study focuses specifically on the recovery of energy during vehicle braking triggered by brake-signal activation, without addressing alternative deceleration strategies under braking conditions. The proposed energy-braking recovery scheme is evaluated primarily through simulation, with the analysis grounded in practical application scenarios and leveraging existing technologies. Firstly, the principle of energy-braking recovery is introduced, and the method of estimating the State of Charge (SOC) of the battery and controlling the motor speed is determined. Then, the simulation model of the energy brake recovery system is built with MATLAB R2023b (MathWorks, Natick, MA, USA), and the design ideas and specific structures of the three modules of the simulation model are introduced in detail. Finally, the results of the simulated motor speed and SOC value of the battery are analysed, and it is confirmed that they meet the requirements of the system and achieve close to the ideal effect.

Keywords: energy-braking recovery; ampere-hour integration (AHI); proportional; integral; derivative (PID) control; MATLAB



Academic Editor: Xiaoxi Liu

Received: 28 June 2025

Revised: 18 August 2025

Accepted: 20 August 2025

Published: 22 August 2025

Citation: Xu, L.; Li, W.; Zhao, Z.; Meng, F. Fast Energy Recovery During Motor Braking: Analysis and Simulation. *J. Low Power Electron. Appl.* **2025**, *15*, 49. <https://doi.org/10.3390/jlpea15030049>

Copyright: © 2025 by the authors. Licensee MDPI, Basel, Switzerland. This article is an open access article distributed under the terms and conditions of the Creative Commons Attribution (CC BY) license (<https://creativecommons.org/licenses/by/4.0/>).

1. Introduction

With the deepening of industrialisation and urbanisation, the number of vehicles in cities is increasing. In urban road conditions, vehicles will brake frequently during driving to adapt to frequent traffic lights and other conditions [1]. The traditional braking method uses the friction of the brake pads to convert the mechanical energy of the vehicle into thermal energy during the driving process, thereby reducing the speed of the vehicle. This method will undoubtedly cause the thermal decay of the brake pads, resulting in a significant reduction in the life of the brake pads [2]. In addition, this method also increases the fuel consumption and exhaust emissions of the vehicle. Relevant studies have confirmed that about a third to a half of the energy consumption of vehicles during driving is lost during braking [3,4]. At the same time, current energy and environmental problems are becoming more and more serious, so it is particularly important to study the recovery of energy braking in order to recover the braking energy of vehicles.

In the research of energy-braking recovery, the relevant research abroad has been relatively mature and perfect. In the early 21st century, the first generation of energy brake recovery systems developed by Honda in Japan realised a certain energy brake recovery with the help of the control strategy of the dual brake power distribution coefficient. Subsequent improvements in the second- and third-generation systems further replaced friction braking with regenerative braking, increasing the amount of energy recovered. At the same time, the Ford Company in the United States developed a wire-transmitted electro-hydraulic braking system, which significantly improved the braking performance compared with the previous mechanical and hydraulic braking systems [5]. With the deepening of research on energy brake recovery, in 2017, Chougale and Lakade et al. studied the energy brake recovery system driven by a brushless DC motor and used fuzzy control and proportional, integral, and derivative (PID) control to obtain a constant braking torque in the system, thus recovering the braking energy of the vehicle [6,7]. In 2023, Hwang and Lee et al. applied an AI algorithm to the energy brake recovery system, which made the system adopt an artificial neural network as the control strategy during braking so as to recover the braking energy and ensure ride comfort [8].

On the domestic side, most of the current research stays in the theoretical analysis or modelling simulation, and there is a lack of product research [3]. In 2013, Ref. [9] deeply studied the conditions and characteristics of energy recovery of the split moment hybrid power system, and constructed constraint equations such as the speed and torque in the process of energy brake recovery through a power split analysis, and, finally, obtained the specific characteristics of energy brake recovery under different working conditions. In 2020, Ref. [10] studied the energy flow mechanism of the vehicle and then constructed a mathematical model that correlated the power consumption, driving conditions, and energy recovery ratio of the vehicle. Based on this, they analysed the energy-saving potential of various models under different operating conditions. In 2021, Ref. [11] built an energy brake recovery system for electric vehicles at the vehicle level, then developed an electronic brake booster, and formulated a control strategy for it [12]. The results show that this booster has a good energy recovery effect, and the driving mileage contribution is up to 15%.

2. Principle of Energy Braking Recovery

The energy brake recovery system is designed to convert part of the mechanical energy released by the vehicle during deceleration or braking into electrical energy through the energy converter, which is then stored in the vehicle battery, and the recovered braking energy can be used as subsequent drive energy, thereby improving the vehicle's endurance. At the same time as braking, energy recovery and reuse are realised [13]. The energy braking recovery system developed in this paper is composed of three parts: the motor, converter, and battery. The motor generates torque during braking, and the converter is responsible for energy conversion to realise the mutual conversion between mechanical energy and electric energy. The battery is used to store the converted energy.

$$SOC = \frac{Q_t}{Q_{max}} * 100\% \quad (1)$$

Since the converted energy is stored in the battery, the main basis for verifying the effect of energy recovery during braking is the battery's state of charge. The state of the battery charge is usually expressed as a percentage, as shown in Formula (1), where Q_t represents the capacity of the battery at the current time, and Q_{max} represents the maximum capacity of the battery. An SOC (State of Charge) of 0 indicates that the battery is fully discharged, and an SOC of 100% indicates that the battery is fully charged.

2.1. SOC Estimation Method

Since the SOC involves the measurement of the battery voltage and temperature and also takes into account the relevant parameters of the battery, the SOC is difficult to directly measure, so it is necessary to adopt an estimation algorithm to obtain the SOC [14,15]. There are several algorithms commonly used to estimate the SOC:

(1) Open-circuit voltage (OCV). This method is one of the earliest SOC estimation methods. The open-circuit voltage refers to the potential difference between the positive and negative terminals when the battery is in an open state and reaches balance. At a certain temperature, the OCV and SOC have a numerically one-to-one corresponding relationship and have a relatively fixed functional relationship, so the SOC can be estimated by the value of the OCV. However, to obtain an accurate OCV value, the battery needs to be disconnected for a certain time before the test to make it stable, so it is difficult to use in the battery charging and discharging process.

(2) Ampere-hour integration (AHI). This method is the simplest SOC estimation method at present. It estimates the current SOC by calculating the amount of electricity charged and discharged in the battery charging and discharging process [16]. The amount of electricity entering the battery during charging increases the SOC, and the amount of electricity exiting the battery during discharging decreases the SOC, as shown in Equation (2), where SOC_{now} represents the initial state of the charge state; η indicates the battery charging efficiency, and the value is usually 1. t represents the current moment; and I indicates the battery charging current.

$$SOC = SOC_{now} + \frac{1}{Q_{max}} \int_0^t \eta I dt \quad (2)$$

As can be seen from the above formula, the ampere-hour integration method is an open-loop system, which does not have the ability to correct the initial value and adjust the deviation in the measurement process, which will cause the accumulation of errors and seriously affect the estimation accuracy of the SOC [17]. In addition, the ampere-hour integration method mainly calculates the increase or decrease in battery power based on the current, which puts forward higher requirements for the accuracy of the current and needs a sufficient current accuracy to ensure the estimation accuracy of the SOC. The advantage of the ampere-hour integration method is that it can be applied to all batteries and has strong applicability, so this method is the most widely used.

(3) The Kalman filter method. This method is based on the state space model of the current system, the initial state value, and the statistical characteristics of noise, and uses the observed output data to correct the system state variables through the principle of the minimum mean square error and then obtains the optimal value of the estimated quantity. Because the observed output data is also affected by the system noise, the optimal estimation can be said to be a filtering process. The typical Kalman filtering method needs to satisfy the model of Equations (3) and (4).

$$x_k = Ax_{k-1} + Bu_{k-1} + w_{k-1} \quad (3)$$

$$z_k = Hx_k + v_k \quad (4)$$

x_k is the state variable of the system; u_k is the input variable of the system; and w_k is the process excitation noise of the system. A is the state transition matrix; B is the parameter matrix of Equation (3); and z_k is the observed variable of the system. v_k is the system's observation noise. H is the parameter matrix of Equation (4).

Using the Kalman filter method to estimate the SOC, the error value can be corrected well so as to effectively improve the estimation accuracy. However, this method largely

depends on the accuracy of the constructed battery model, and it is a challenging task to build a high-precision battery model, so this method has not been widely promoted and applied.

(4) The neural network method. In this method, a precise neural network model is established to simulate the dynamic characteristics of the battery, so as to estimate the SOC of the battery. Neural networks are generally divided into the input layer, intermediate layer, and output layer, and the input layer of the SOC generally includes the current, voltage, and battery-related information, which is determined by practical problems. The advantage of this method is that it does not need to specify the exact relationship between the input and output in advance, and this relationship can be gradually established in the subsequent training process, and the method has the characteristics of self-adaptation. However, its disadvantage is that the training process requires a huge amount of data support, which leads to a long training cycle, and the training method used has a greater impact on the estimation accuracy.

2.2. PID Control Method

PID control, namely, proportional, integral, and derivative control, is a control algorithm commonly used in industrial systems. It has the advantages of simple principles, an easy adjustment, and a wide application range, and it can quickly and accurately correct the negative feedback system. Therefore, the PID module is designed in the energy braking recovery system to better regulate the speed of the system. PID control can increase the precision of the control by adjusting the coefficients of the three links—ratio (P), integral (I), and differential (D)—in which the proportion link affects the response speed of the system to the error, and the integration link is responsible for eliminating the static error of the system; The differential link can be adjusted in advance to ensure the stability of the system [18,19]. The PID control principal diagram is shown in Figure 1.

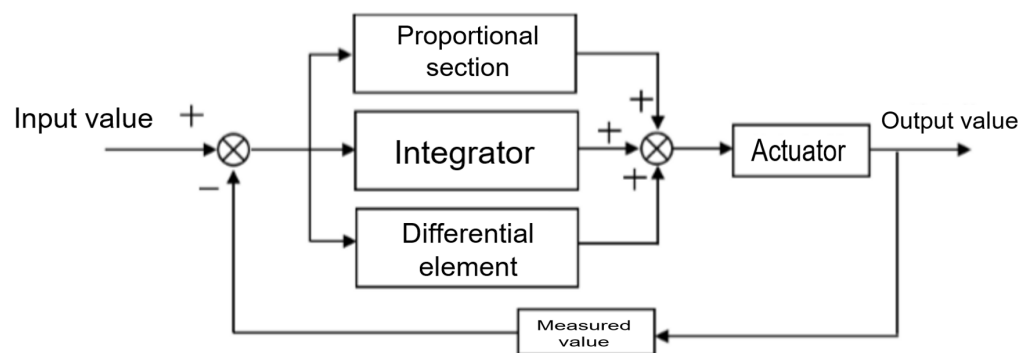


Figure 1. PID control schematic diagram.

The input value $e(t)$ of PID control is the difference between the target value of the control quantity and the measured value, and the output value $u(t)$ is shown in Equation (5), where t is the system time, K_p is the proportional coefficient, K_i is the integral coefficient, and K_d is the differential coefficient.

$$u(t) = K_p e(t) + K_i \int_0^t e(\tau) d\tau + K_d \frac{de(t)}{dt} \quad (5)$$

Based on the above principle, PID control can be used to adjust the motor speed, bus current, and bus voltage in the energy brake recovery system so as to meet the relevant requirements of the system.

3. Simulation of Energy Brake Recovery

In order to verify the feasibility of the above energy brake recovery system, this paper uses the Simulink toolbox of MATLAB software to build a simulation model and conduct a feasibility analysis [20]. The energy brake recovery system model built in this paper consists of a main module, a control module, and a recovery module. Each module will be introduced in the following sections.

In this study, the primary focus is on energy recovery from the motor after braking, rather than the braking process itself. Braking is considered a prerequisite for the energy recovery study. The braking signal, along with other relevant information, is directly transmitted from the motorcycle's ECU to the motor controller. As such, this study does not delve deeply into the specifics of the braking system or process. Instead, we use a triggering signal to simulate the braking action and employ PID control to model the reduction in motor speed during braking. This approach allows us to focus on the energy recovery aspect after braking.

3.1. Main Module

The main structure of the main module includes the battery, the inverter bridge, and the motor. The DC output of the battery is converted to the AC output of the driving motor through the inverter bridge. After the motor is started, the speed, torque, and phase current will be output to the control module and recovery module to ensure its normal operation [21,22]. The specific structure is shown in Figure 2.

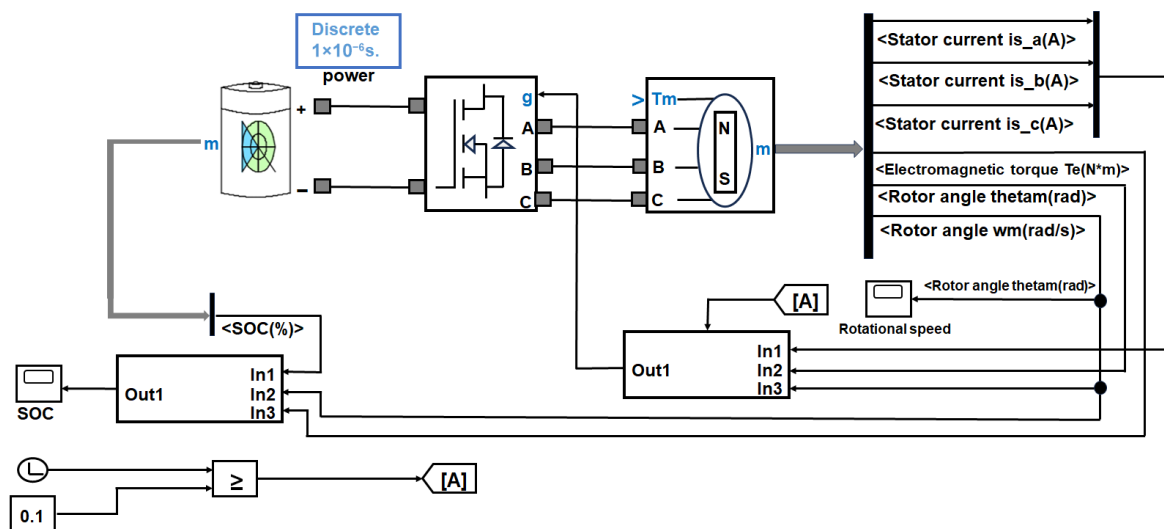


Figure 2. Body module structure diagram.

The motor model in this module uses a brushless DC motor, which has a relatively simple structure, good heat dissipation performance, and high power density [23], and the specific parameters are shown in Table 1. In this simulation model, the parameters like stator winding resistance, flux linkage, and inductance are set to the default values from the Simulink toolbox for simplicity. These values will be adjusted according to the actual motor specifications in future work. The study is focused on a motorcycle, and the 12 V BLDC motor used in this simulation is a voltage that has been chosen accordingly.

Table 1. Motor parameter.

Parameter	Value
Operating voltage	12 V
Rated speed	2000 rpm
Number of poles	6
Hall installation angle	120°

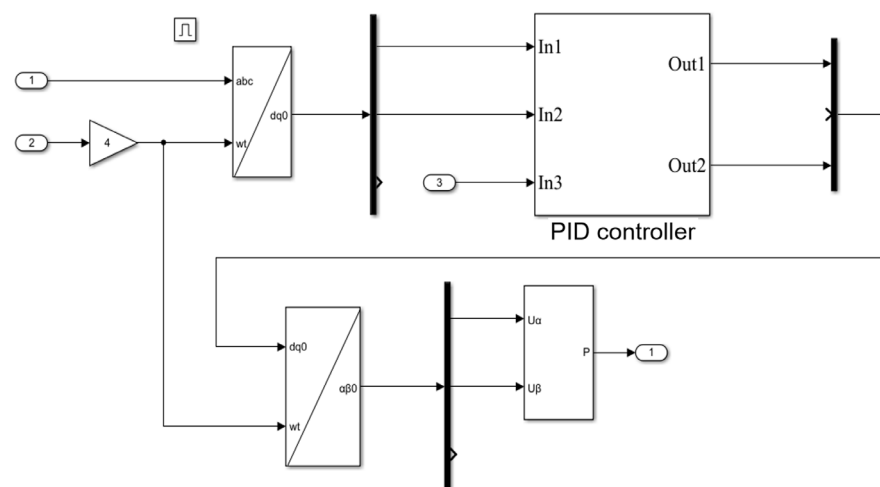
The battery model is based on the parameters of the motor model, and the common vehicle battery is selected. The specific parameters are shown in Table 2, while other components, including the inverter, use the default parameters from the Simulink toolbox.

Table 2. Battery parameters.

Parameter	Value
Battery voltage	12 V
Battery capacity	6 Ah
Current (Stationary Charging)	≤ 0.6 A
Current (Motor Acceleration)	≤ 90 A
Current (Regenerative Braking)	≤ 20 A

3.2. Control Module

The control module is based on the PID control method introduced in the previous section to control the motor. The input value of this module is the three-phase current of the motor, the angle of the motor, and the speed of the motor, and the output value is the PWM signal to stabilise the speed of the motor at the target value [24,25]. The specific structure is shown in Figure 3. The inputs 1, 2, and 3 in Figure 3 correspond to In1, In2, and In3 in Figure 2, which represent the system control signals. The desired value is set within the PID control block itself. The block's inputs include the current motor speed and the transformed current obtained through the system, while the output is the adjusted current after PID control. The Gain Block 4 is used to convert the input motor angle for further processing in the control system. In the current simulation model, a delay module has been implemented, with the motor starting at $t = 0.1$ s.

**Figure 3.** Control module structure diagram.

This module first transforms the input three-phase current from the stationary ABC reference frame to the rotating dq reference frame. The angle position of the rotating frame is determined by the angle of the input motor. The resulting current will be used as the input value for the subsequent PID calculation.

Clarke Transformation: We transform the phase currents i_a , i_b , and i_c from the stationary abc frame to the stationary $\alpha\beta$ frame:

$$i_\alpha = i_a \quad (6)$$

$$i_\beta = \frac{i_a}{\sqrt{3}} + \frac{2i_b}{\sqrt{3}} \quad (7)$$

Park Transformation: We then transform the currents i_α and i_β from the stationary $\alpha\beta$ frame to the rotating dq frame:

$$i_d = i_\alpha \cos\theta + i_\beta \sin\theta \quad (8)$$

$$i_q = -i_\alpha \sin\theta + i_\beta \cos\theta \quad (9)$$

where θ is the rotor angle.

In PID control, the input value of the PID controller is the target speed value, the current motor speed, and the current obtained by the transformation. After a series of PID calculations, the output value of the PID controller is input into the PWM generator, and then the space vector pulse width modulation technology is used to generate the required PWM signal, and, finally, the obtained PWM signal is input into the inverter bridge, so as to realise the speed control of the motor. In our study, the PID parameters were tuned so that the system operates in a critically damped state, which effectively avoids oscillations while maintaining a fast dynamic response. This explains why no dynamic oscillations appear in the simulation results.

3.3. Recovery Module

The battery model used in this simulation model can directly output the real-time SOC value of the battery, which can correct the measurement deviation generated in the process of using the ampere-hour integration method, so as to eliminate the error in time and ensure the SOC estimation accuracy. Based on this, the recovery module adopts the ampere-hour integration method as the SOC estimation method and designs two parts: the charging current calculation and SOC estimation. The specific structure is shown in Figure 4.

According to the ampere-hour integration principle introduced in the previous section, this module mainly uses the charging current to calculate the battery power change during charging and discharging. From the relationship between power and speed and torque and the relationship between power and current and voltage, the formula of the charging current can be derived, as shown in Equation (10), where T is the motor torque, n is the motor speed, and U is the battery terminal voltage [26]. Equation (10) is derived based on the principle of conservation of energy, specifically from the conversion between mechanical energy and electrical energy. As this study is a theoretical simulation, we have neglected losses for the sake of simplification.

$$I = \frac{T_n}{9550U} \quad (10)$$

The charging current accuracy obtained by the above method is higher, and the SOC estimation accuracy can be better guaranteed. After the charging current is obtained, it and the real-time SOC value of the battery are input into the SOC estimation part, and then the

SOC value after charging can be calculated according to the formula of the ampere-hour integration method so as to determine the effect of energy recovery.

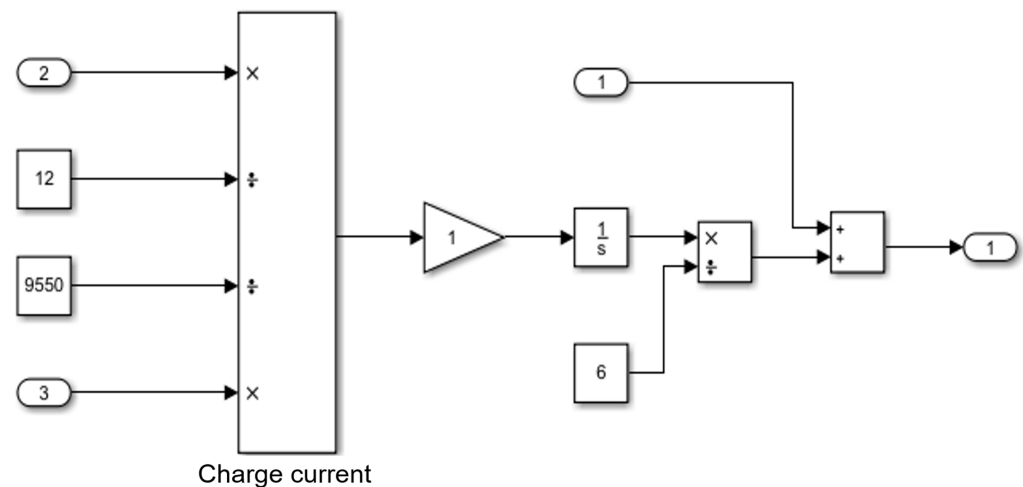


Figure 4. Control module reclaim diagram.

3.4. Analysis of Simulation Results

After the simulation model of the energy brake recovery system is built, the model is initialised first, then the simulation model is run, and the operation results are analysed. The model initialisation mainly sets the initial value of each module, sets the simulation time to 2 s, and sends the brake signal at 1 s. The initial speed of the motor is set to the rated speed of 2000 rpm, and the speed after braking is set to 1000 rpm. In order to ensure that the energy is fully recovered during braking and will not be limited by battery saturation, the initial SOC value of the battery is set to 40%.

After starting the motor and adjusting the control module, the motor speed is stabilised at 2000 rpm. Then, when $t = 1$ s, the braking signal comes, the model enters the braking state, and the motor speed drops to 1000 rpm. The change in motor speed in the simulation process is shown in Figure 5. As can be seen from the figure, the simulation model has a good ability to regulate the speed of the motor so that it can reach the target speed in a short time and maintain stability at the target speed.

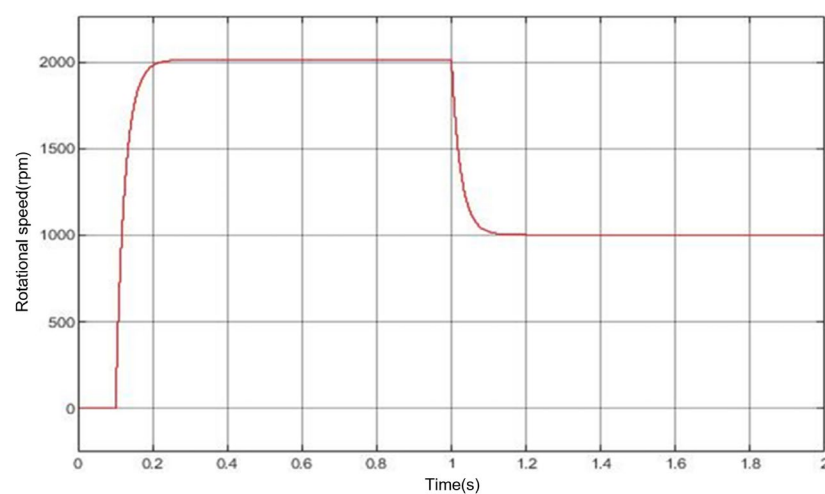


Figure 5. Motor rotational speed.

The motor is not operating within the constant torque region of its characteristic curve. The current simulation model mainly focuses on the motor's performance at the rated speed

and below, without considering the corner speed or field-weakening algorithms. Figure 6 shows the torque variation curve. We acknowledge the importance of considering the full operating range, including the transition beyond the corner speed. In future work, we plan to extend the simulation to cover a broader speed range to better evaluate the motor's performance under various conditions. We have not implemented a field-weakening algorithm in this model. Instead, we employ a PID controller to adjust the PWM signals, which, in turn, control the three-phase currents supplied to the motor, affecting both the speed and torque.

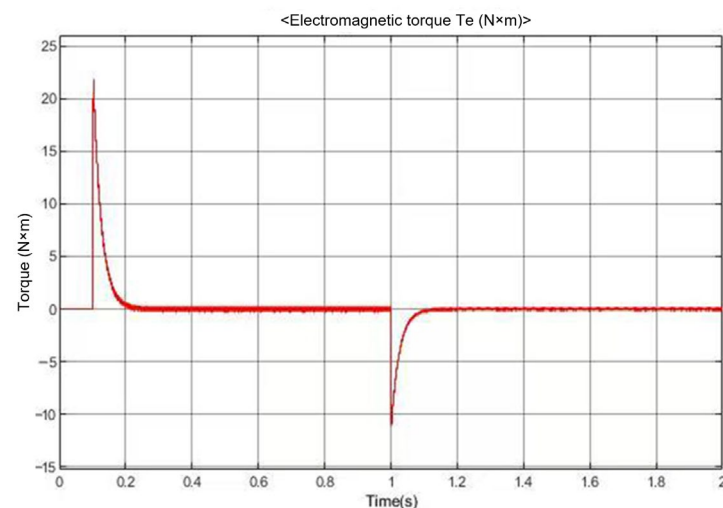


Figure 6. Torque variation curve.

In the current simulation model, the motor operates under no-load conditions, whereas, in the actual operation of the motorcycle under study, the motor exhibits a rated operating current of 20 A and a peak operating current of up to 90 A. The current curve shown in Figure 7 represents the charging current of the recovery module, not the motor's operating current. Regarding the battery, the 0.1 C charging current corresponds to the battery's typical charging rate when using a standard charger, with a charging time of approximately 10–12 h. This is a simplified assumption for the simulation, and we acknowledge that it may not fully reflect the real-world charging dynamics for higher-power applications.

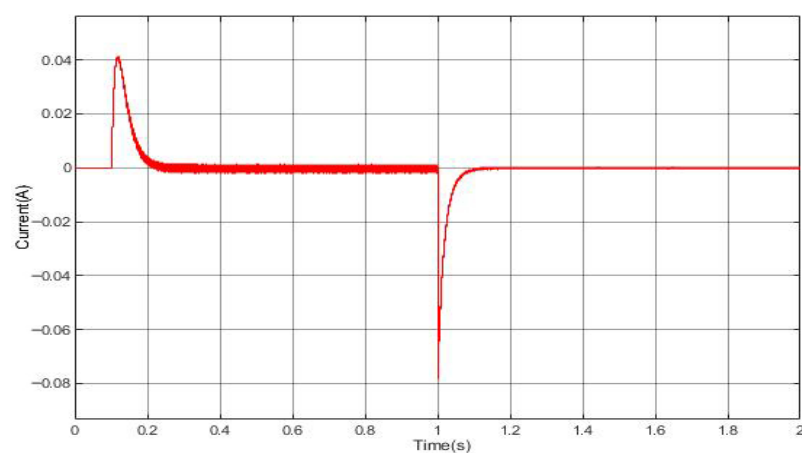


Figure 7. The charging current profile of the recovery module exhibits.

After the initial SOC value of the battery and the speed and torque of the motor are input, the recovery module starts to run, and its changes in the simulation process are

shown in Figure 8. As can be seen from the figure, when the motor is not started, the battery SOC remains 40% unchanged; when the motor starts to accelerate to the rated speed, the SOC also begins to decrease rapidly until the motor speed stabilises at the rated speed, at which time the SOC slowly decreases to maintain the speed.

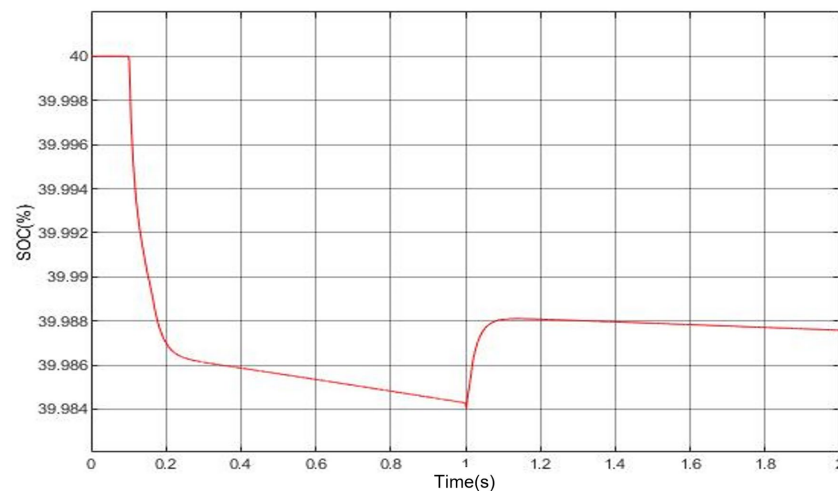


Figure 8. Battery SOC changing characteristic.

When the braking signal comes, the motor speed starts to drop, the SOC stops falling and starts to rise, indicating that the recovery module starts to function, and the energy during braking is recovered to the battery [27]. As the motor speed stabilises at the braking speed, the SOC also stops rising, indicating that the braking process has ended at this time, and no energy can be recovered. Then, in order to overcome the motor operation resistance, the SOC began to decline slowly again.

From the above simulation results, it can be seen that, when the motor speed drops, the SOC of the battery rises correspondingly, which indicates that part of the mechanical energy during braking is converted into electrical energy. The simulation model built in this paper can realise the function of energy-braking recovery. The simulation model employed in this study is a simplified variant derived from the research vehicle platform, representing an optimised abstraction of the existing physical motorcycle configuration.

3.5. Analysis of Test Results

The simulation model development has currently reached the no-load stage. However, practical tests were conducted to characterise the actual charge/discharge behavior during motor operation. For the studied motorcycle battery system, the charger delivers a 0.1 C charging current during stationary charging. Manufacturer specifications dictate the operational limits of a ≤ 90 A discharge current during motor acceleration and a ≤ 20 A charging current during regenerative braking. Experimental measurements of the starting current shown in Figure 9 were acquired using a current probe with 5 mV/A sensitivity and oscilloscope $10\times$ magnification, establishing a 1 V-to-20 A conversion ratio. The recorded peak starting current of 81.6 A confirms the compliance with the discharge current requirement, while separate tests verified that regenerative charging currents remained within the 20 A threshold.



Figure 9. Starting current diagram of actual motor operation.

4. Conclusions

This paper mainly studies the energy-braking recovery method. This work is application-oriented, aiming to apply existing technologies in a practical vehicle braking scenario. The main contribution of this paper is to demonstrate, through simulation, the feasibility of regenerative braking energy recovery under these conditions, which serves as a foundation for future hardware implementation. Firstly, the principle of energy braking recovery is introduced, and the method of estimating the battery SOC and controlling the motor speed is determined. Then, the Simulink toolbox in MATLAB software is used to build the simulation model of the energy brake recovery system, including the main module, control module, and recovery module, and then the design ideas and specific structures of the above three modules are introduced in detail [28]. After building the simulation model of the system, this paper analyses the results of the simulated motor speed and battery SOC value, confirming that they meet the requirements of the system and achieve the ideal effect. After that, the energy brake recovery method will be applied to motor vehicles to help them further save energy, reduce emissions, and promote green development [29]. Further integration with smart grids may unlock additional energy-saving potential [30]. This study will be extended to investigate other types of energy storage devices in future research, such as supercapacitors, which will be explored in more detail.

Author Contributions: Conceptualisation, F.M. and L.X.; methodology, F.M. and L.X.; software, L.X.; validation, L.X.; writing—original draft preparation, L.X. and W.L.; writing—review and editing, F.M. and Z.Z.; supervision, F.M.; project administration, L.X. All authors have read and agreed to the published version of the manuscript.

Funding: This research received no external funding.

Institutional Review Board Statement: Not applicable.

Informed Consent Statement: Not applicable.

Data Availability Statement: The original contributions presented in this study are included in this article. Further inquiries can be directed to the corresponding author.

Conflicts of Interest: Author Lin Xu is affiliated with the 13th Research Institute, China Electronics Technology Group Corporation. The remaining authors declare that the research was conducted in the absence of any commercial or financial relationships that could be construed as a potential conflict of interest.

References

- Heydari, S.; Fajri, P.; Rasheduzzaman, M. Maximizing regenerative braking energy recovery of electric vehicles through dynamic low-speed cutoff point detection. *IEEE Trans. Transp. Electr.* **2019**, *5*, 262–270. [\[CrossRef\]](#)
- Hardman, S.; Chandan, A.; Tal, G. The effectiveness of financial purchase incentives for battery electric vehicles—A review of the evidence. *Renew. Sustain. Energy Rev.* **2017**, *80*, 1100–1111. [\[CrossRef\]](#)
- Zhang, J.; Wang, Z.; Liu, P.; Zhang, Z. Energy consumption analysis and prediction of electric vehicles based on real-world driving data. *Appl. Energy* **2020**, *275*, 115408. [\[CrossRef\]](#)
- Lv, S.; Li, X. A Review of Regenerative Braking Energy Recovery Research for Pure Electric Vehicles. In Proceedings of the 2024 IEEE 5th International Conference on Advanced Electrical and Energy Systems (AEES), Lanzhou, China, 29 November–1 December 2024; pp. 468–472.
- Ko, J.; Ko, S.; Son, H. Development of brake system and regenerative braking cooperative control algorithm for automatic-transmission-based hybrid electric vehicles. *IEEE Trans. Veh. Technol.* **2014**, *64*, 431–440. [\[CrossRef\]](#)
- Chougale, R.G.; Lakade, C.R. Regenerative braking system of electric vehicle driven by brushless DC motor using fuzzy logic. In Proceedings of the 2017 IEEE International Conference on Power, Control, Signals and Instrumentation Engineering (ICPCSI), Chennai, India, 21–22 September 2017; IEEE: Chennai, India, 2017; pp. 2167–2171.
- Satzger, C.; de Castro, R.; Bünte, T. A model predictive control allocation approach to hybrid braking of electric vehicles. In Proceedings of the 2014 IEEE Intelligent Vehicles Symposium Proceedings, Dearborn, MI, USA, 8–11 June 2014; pp. 286–292.
- Hwang, M.H.; Lee, G.S.; Kim, E.; Kim, H.W.; Yoon, S.; Talluri, T.; Cha, H.R. Regenerative braking control strategy based on AI algorithm to improve driving comfort of autonomous vehicles. *Appl. Sci.* **2023**, *13*, 946. [\[CrossRef\]](#)
- Zhang, H.; Wang, H. Braking energy recuperation performance of input coupled power-split hydraulic hybrid powertrain. *Trans. Chin. Soc. Agric. Eng.* **2013**, *29*, 23–30.
- Zhou, J.; Lu, D.; Yi, F.; Shen, Y.; Lin, H.; Yang, T. Research on Control Strategy of Flywheel Energy Storage Pure Electric Vehicle Braking Energy Recovery System. In Proceedings of the 2020 4th CAA International Conference on Vehicular Control and Intelligence (CVCI), Hangzhou, China, 18–20 December 2020; pp. 536–542.
- Yang, Z.; Tan, G.; Ling, H.; Zeng, P.; Li, C.; Liu, L. Research on braking energy recovery strategy of pure electric vehicle. In Proceedings of the Brake Colloquium & Exhibition—39th Annual, Orlando, FL, USA, 17–20 October 2021; Technical Paper; SAE: Warrendale, PA, USA, 2021; Volume 1, p. 1264.
- Duong, T.-T.; Huynh, P.-S.; Ngo, Q.-T. Research to Evaluate the Regenerative Braking System Effect on Fuel Consumption of Hybrid Vehicle. In Proceedings of the 2021 International Conference on System Science and Engineering (ICSSE), Ho Chi Minh City, Vietnam, 26–28 August 2021; pp. 252–256.
- Yuan, X.; Li, L.; Gou, H.; Dong, T. Energy and environmental impact of battery electric vehicle range in China. *Appl. Energy* **2015**, *157*, 75–84. [\[CrossRef\]](#)
- Fu, S.; Lyu, T.; Min, F.; Luo, W.; Luo, C.; Wu, L.; Xie, J. Review of estimation methods on SOC of lithium-ion batteries in electric vehicles. *Energy Storage Sci. Technol.* **2021**, *10*, 1127–1136. [\[CrossRef\]](#)
- Chen, G.; Jiang, S.; Xie, M.; Yang, F. A hybrid DNN-KF model for real-time SOC estimation of lithium-ion batteries under different ambient temperatures. In Proceedings of the 2022 Global Reliability and Prognostics and Health Management (PHM-Yantai), Yantai, China, 13–16 October 2022; pp. 1–5.
- Labiri, H.; Farhat, S.; Nadir, E.; Chekoubi, Z.; Elihssini, H. SoC Estimation in Electric Cars using Ampere-Hour and Fuzzy Logic Approaches. In Proceedings of the 2025 5th International Conference on Innovative Research in Applied Science, Engineering and Technology (IRASET), Fez, Morocco, 15–16 May 2025; pp. 1–4.
- Zhu, D.; Chikkannanavar, S.; Tao, J. SOC Estimation Error Analysis for Li Ion Batteries. In Proceedings of the 2021 IEEE Transportation Electrification Conference & Expo (ITEC), Chicago, IL, USA, 21–25 June 2021; pp. 479–483.
- Doicin, B.; Popescu, M.; Patrascioiu, C. PID Controller optimal tuning. In Proceedings of the 2016 8th International Conference on Electronics, Computers and Artificial Intelligence (ECAI), Ploiesti, Romania, 30 June–2 July 2016; pp. 1–4.
- Chen, W.; Du, Z. Nonlinear adaptive control with integral-PID adaptive law. In Proceedings of the 29th Chinese Control Conference, Beijing, China, 29–31 July 2010; pp. 2125–2128.
- Yue, X.L.; Bai, P. Modeling and Simulation of Brushless DC Motor Speed Control System Based on MATLAB/SIMULINK. *Adv. Mater. Res.* **2014**, *998*, 755–758. [\[CrossRef\]](#)
- Long, B.; Lim, S.T.; Ryu, J.H.; Chong, K.T. Energy-regenerative braking control of electric vehicles using three-phase brushless direct-current motors. *Energies* **2013**, *7*, 99–114. [\[CrossRef\]](#)
- Kumar, D.; Gupta, R.A.; Gupta, N. Modeling and simulation of four switch three-phase BLDC motor using anti-windup PI controller. In Proceedings of the 2017 Innovations in Power and Advanced Computing Technologies (i-PACT), Vellore, India, 21–22 April 2017; pp. 1–6.

23. Cheng, J.; Zhang, G.; Lu, C.; Wu, C.; Xu, Y. Research of brushless DC motor control system based on RBF neural network. In Proceedings of the 2017 32nd Youth Academic Annual Conference of Chinese Association of Automation (YAC), Hefei, China, 19–21 May 2017; IEEE: Hefei, China, 2017; pp. 521–524.
24. Wang, P.; Duan, X.; Chen, C.; Liu, S. Experimental investigation on the exhaust emissions and performance of a hybrid electric motor coupled with an energy recovery system. *Case Stud. Therm. Eng.* **2023**, *45*, 102994. [[CrossRef](#)]
25. Dasi, S.; Sandiri, R.; Anuradha, T.; Sri, T.S.; Majji, S.; Murugan, K. The State-of-the-art Energy Management Strategy in Hybrid Electric Vehicles for Real-time Optimization. In Proceedings of the 2023 International Conference on Inventive Computation Technologies (ICICT), Lalitpur, Nepal, 26–28 April 2023; pp. 1637–1643.
26. Abraham, P.K.; Namboodiry, J. Ultracapacitor based Constant Torque Regenerative Braking System for a Brushless DC Motor. In Proceedings of the 2021 IEEE International Power and Renewable Energy Conference (IPRECON), Kollam, India, 24–26 September 2021; IEEE: Kollam, India, 2021; pp. 1–5.
27. Shi, C.; Wang, W.; Li, W. Analysis of Evaluation Indicators for Regenerative Braking Energy Recovery in Hybrid Electric Vehicles. In Proceedings of the 2025 IEEE 8th Information Technology and Mechatronics Engineering Conference (ITOEC), Chongqing, China, 14–16 March 2025; pp. 952–957.
28. Sakai, M.; Takeshita, T. Power Control Using Sub-Battery for Electric Motorcycle. In Proceedings of the 2024 27th International Conference on Electrical Machines and Systems (ICEMS), Fukuoka, Japan, 26–29 November 2024; pp. 3757–3762.
29. Szumska, E.M. Regenerative Braking Systems in Electric Vehicles: A Comprehensive Review of Design, Control Strategies, and Efficiency Challenges. *Energy* **2025**, *18*, 2422. [[CrossRef](#)]
30. Abdelfattah, W.; Abdelhamid, A.S.; Hasanien, H.M.; Rashad, B.A.-E. Smart Vehicle-to-Grid Integration Strategy for Enhancing Distribution System Performance and Electric Vehicle Profitability. *Energy* **2024**, *302*, 131807. [[CrossRef](#)]

Disclaimer/Publisher’s Note: The statements, opinions and data contained in all publications are solely those of the individual author(s) and contributor(s) and not of MDPI and/or the editor(s). MDPI and/or the editor(s) disclaim responsibility for any injury to people or property resulting from any ideas, methods, instructions or products referred to in the content.